

## Glycosylated Nanoparticles as Efficient Antimicrobial Delivery Agents

Ahmed M. Eissa,<sup>a,b,c,d</sup> \* Ali Abdulkarim,<sup>a</sup> Gary J. Sharples,<sup>e</sup> Neil R. Cameron<sup>a,b,c</sup> \*

<sup>a</sup> Department of Chemistry, University of Durham, South Road, Durham, DH1 3LE, U.K.

<sup>b</sup> School of Engineering, University of Warwick, Coventry, CV4 7AL, U.K.

<sup>c</sup> Department of Materials Science and Engineering, Monash University, Clayton 3800, Victoria, Australia.

<sup>d</sup> Department of Polymers, Chemical Industries Research Division, National Research Centre (NRC), El-Bohoos Street, Dokki, Cairo, Egypt.

<sup>e</sup> School of Biological and Biomedical Sciences, Biophysical Sciences Institute, Department of Chemistry, University of Durham, Durham DH1 3LE, U.K.

Synthetic polymer nanoparticles that can be tailored through multivalent ligand display on the surface, while at the same time allowing encapsulation of desired bioactive molecules, are especially useful in providing a versatile and robust platform in the design of specific delivery vehicles for various purposes. Glycosylated nanoparticles (glyco-NPs) of a poly(*n*-butyl acrylate) (pBA) core and poly(N-2-( $\beta$ -D-Glucosyloxy)ethyl acrylamide) (p(N $\beta$ GlcEAM)) or poly(N-2-( $\beta$ -D-galactosyloxy)ethyl acrylamide) (p(N $\beta$ GalEAM)) corona were prepared *via* nanoprecipitation in aqueous solutions of preformed amphiphilic glycopolymers. Well-defined block copolymers

1  
2  
3 of (poly(pentafluorophenyl acrylate) (pPFPA) and pBA were first prepared by RAFT  
4  
5 polymerization followed by post-polymerization functionalization with aminoethyl glycosides to  
6  
7 yield p(N $\beta$ GlcEAM-*b*-BA) and p(N $\beta$ GalEAM-*b*-BA) which were then used to form glyco-NPs  
8  
9 (glucosylated and galactosylated NPs, Glc-NPs and Gal-NPs, respectively). The glyco-NPs were  
10  
11 characterized by dynamic light scattering (DLS) and TEM. Encapsulation and release of  
12  
13 ampicillin, leading to nanoparticles that we have termed ‘glyconanobiotics’, were studied. The  
14  
15 ampicillin-loaded glyco-NPs were found to induce aggregation of *Staphylococcus aureus* and  
16  
17 *Escherichia coli* and resulted in antibacterial activity approaching that of ampicillin itself. This  
18  
19 glyconanobiotics strategy represents a potential new approach for the delivery of antibiotics  
20  
21 close to the surface of bacteria by promoting bacterial aggregation. Defined release in the  
22  
23 proximity of the bacterial envelope may thus enhance antibacterial efficiency and potentially  
24  
25 reduce the quantities of agent required for potency.  
26  
27  
28  
29  
30  
31  
32  
33  
34  
35  
36  
37  
38  
39  
40  
41  
42  
43  
44  
45  
46  
47  
48  
49  
50  
51  
52  
53  
54  
55  
56  
57  
58  
59  
60

1  
2  
3 Over the last century, morbidity and mortality as a consequence of infectious diseases have  
4 decreased drastically, due to the wide-spread development and deployment of vaccines and  
5 antimicrobial agents.<sup>1</sup> However, bacterial resistance to our available antibiotic repertoire is now  
6 reaching a critical level, potentially bringing about a post-antibiotic era.<sup>2</sup> Considerable effort has  
7 been expended to overcome this problem through the discovery of new antibiotics and chemical  
8 modification of existing antibacterial drugs. Nevertheless, the development of new antimicrobial  
9 drugs is unlikely to outpace the emergence of microbial pathogen resistance. The continued  
10 evolution of antimicrobial resistance mechanisms has prompted the scientific community to seek  
11 longer-term solutions to this ever-growing problem.<sup>3</sup> Metallic nanomaterials (e.g. Ag, Au, and  
12 Cu) have been found to display strong antimicrobial properties.<sup>4</sup> Nevertheless, their applications  
13 as antimicrobial agents are limited by their potential toxicity to human cells as a result of their  
14 unusual physicochemical properties and/or physical or chemical production techniques.<sup>5</sup>  
15 Encapsulation or conjugation of antibiotics into different classes of nanocarriers has been  
16 recently represented as a potential approach to combat infectious diseases.<sup>6-8</sup> This approach can  
17 not only offer efficient intracellular delivery to pathogens but also help in controlling the amount  
18 and frequency of drug dosage and hence reduces the toxicity associated to therapy and may  
19 overcome bacterial resistance.  
20  
21

22 Strategies that do not kill the pathogens yet interfere with their pathogenic mechanisms may  
23 provide a promising alternative. One such strategy is anti-adhesion therapy, which interferes with  
24 the early stages of infection in which pathogens attach to the mammalian cell surface.<sup>9-11</sup> This  
25 adhesion is often mediated by protein-carbohydrate interactions: proteins on the pathogen  
26 binding to displayed carbohydrate structures or receptors on the eukaryotic cell. These  
27 interactions are often highly specific and determine the preference of the pathogen for certain  
28  
29  
30  
31  
32  
33  
34  
35  
36  
37  
38  
39  
40  
41  
42  
43  
44  
45  
46  
47  
48  
49  
50  
51  
52  
53  
54  
55  
56  
57  
58  
59  
60

1  
2  
3 tissue types, known as tropism. Free carbohydrates can be harnessed to interfere with bacterial  
4 attachment, thus preventing initial colonization and subsequent infection. This principle is  
5 operative daily as part of the innate immune system, for example human breast milk contains  
6 many oligosaccharides that act as anti-adhesives.<sup>12</sup> However, the limited affinity of monovalent  
7 carbohydrates for target proteins that are often multivalent hinders the application of this  
8 approach. Therefore, designing multivalent glycosylated constructs that can inhibit protein-  
9 carbohydrate interactions may be productive in finding a way forward.

19  
20 During the last decade, nanoparticles presenting carbohydrate/glycan functionalities at their  
21 surfaces have been reported to exhibit antibacterial actions towards different classes of bacteria  
22 including Gram-positive, Gram-negative and mycobacteria.<sup>13</sup> Most of these reports focused on  
23 using nanoparticles with an inorganic core, such as gold, silver, iron oxide, silica, copper,  
24 bismuth, palladium, and platinum.<sup>14</sup> A major reason for the special interest in these inorganic  
25 materials is their attractive physical properties, such as plasmonic effects, luminescence and/or  
26 magnetic susceptibility which make them especially useful for both imaging and therapeutic  
27 (theranostic) applications. One of the most studied examples of carbohydrate-mediated targeting  
28 that leads to bacterial growth inhibition exerted by aggregation has been shown with  
29 mannosylated silver and gold nanoparticles, interacting with fimbriated *E. coli* strains.<sup>15, 16</sup>  
30 Bacterial growth inhibition has also been demonstrated with non-targeting glycosylated  
31 nanoparticles, where the carbohydrate moieties serve as stabilising and/or solubilizing agents.  
32 For example, silver nanoparticles functionalized with kocuran (an exopolysaccharide produced  
33 by *Kocuria rosea* strain BS-1) were probed against a range of bacterial strains, of which *S.*  
34 *aureus* was affected the most.<sup>17</sup> The binding affinity and specificity of glycosylated nanoparticles  
35 to many bacterial strains is not well-studied in the literature and needs further attention.

1  
2  
3 Here, we report the construction of polymeric glycosylated nanoparticles (glyco-NPs) that  
4 encapsulate an antibiotic (ampicillin) as an amalgamated system, which we refer to as  
5 *glyconanobiotics*. Our hypothesis is that antibiotic delivery will be enhanced if the nanoparticle  
6 delivery vehicle is capable of binding to, and aggregating, the bacteria, and therefore releasing  
7 the antibiotic in the proximity of the bacterial surface. As an example, the pili of *E. coli* contain  
8 at their tips the FimH protein which has binding specificity for glucose and mannose.<sup>18</sup>  
9  
10 Consequently, multivalent glucosylated nanoparticles loaded with antibacterial agent could form  
11 such a glyconanobiotic delivery system. Ampicillin was used in this study as a well-  
12 characterized and potent antibiotic. It is a semi-synthetic derivative of penicillin, with a relatively  
13 short-term stability in aqueous solutions.<sup>19</sup> It is used clinically for the treatment of a broad range  
14 of bacterial infections.<sup>20, 21</sup> Improvement of its activity and reduction of its allergic and toxic  
15 reactions have been achieved by means of topical formulations<sup>22</sup> and the use of liposomal  
16 nanoparticles as passive delivery systems.<sup>23, 24</sup> Moreover, from the pharmaceutical application  
17 perspective, these liposomal nano-carriers provide endocytozable formulations for intracellular  
18 chemotherapy, since  $\beta$ -lactam antibiotics do not diffuse readily through the lysosomal membrane  
19 because of their ionic character at neutral extracellular or cytoplasmic pH.<sup>25</sup> Polymeric  
20 nanoparticles offer, over liposomes, certain advantageous features with respect to chemical and  
21 biological stability and prolonged circulation times in the bloodstream.<sup>26</sup> Furthermore, they can  
22 be prepared in such a way that they present on their external surface biologically active  
23 functionalities,<sup>27, 28</sup> for example carbohydrates as employed in this study.  
24  
25  
26  
27  
28  
29  
30  
31  
32  
33  
34  
35  
36  
37  
38  
39  
40  
41  
42  
43  
44  
45  
46  
47  
48  
49  
50  
51  
52

## 53 EXPERIMENTAL METHODS

54  
55 *Typical synthesis of amphiphilic glycopolymers*  
56  
57  
58  
59  
60

1  
2  
3 PFPA (476 mg, 2 mmol), benzyl 2-hydroxyethyl carbonotrithioate (32 mg, 0.13 mmol), AIBN  
4 (4.5 mg, 0.025 mmol) and benzene (5 mL) were placed into a Schlenk flask equipped with a  
5 stirrer bar. After degassing by purging with nitrogen under an ice bath for 30 min, the solution  
6 was heated to 70 °C and stirred for 6 h. Conversion of monomer to polymer was determined by  
7 <sup>1</sup>H NMR spectroscopy. The polymerization reaction was quenched by cooling and exposure to  
8 air. n-Butyl acrylate (2.76 g, 21.6 mmol) and AIBN (4.5 mg, 0.025 mmol) in benzene (8 mL)  
9 were added to the crude PFPA homopolymer solution. After degassing by purging with nitrogen  
10 under an ice bath for 30 min, the mixture was heated to 70 °C and stirred for 18 h. After  
11 quenching the reaction, the solvent was removed under reduced pressure and the product was  
12 reprecipitated twice from THF into cold methanol (at 0 °C). The block copolymer was dried  
13 under reduced pressure to yield a yellow powder which was fully characterized by SEC, <sup>1</sup>H and  
14 <sup>19</sup>F NMR spectroscopy, and ATR-FTIR spectroscopy.

15  
16  
17  
18  
19  
20  
21  
22  
23  
24  
25  
26  
27  
28  
29  
30  
31  
32 The obtained PFPA/BA block copolymer was first dissolved in toluene (30 mL) in the  
33 presence of a large excess of AIBN (30 eq.). After degassing by purging with nitrogen under an  
34 ice bath for 30 min, the mixture was heated to 70 °C and stirred for 6 h. After quenching the  
35 reaction, the solvent was removed under reduced pressure and the product was reprecipitated  
36 from THF into cold methanol (at 0 °C) to yield p(PFPA<sub>15</sub>-*b*-BA<sub>120</sub>) as an off-white powder. 2'-  
37 aminoethyl-β-D-glucopyranoside (100 mg, 0.45 mmol) was mixed with triethylamine (100 μL) in  
38 water (1 mL). While stirring, the sugar solution was added slowly to p(PFPA<sub>15</sub>-*b*-BA<sub>120</sub>) (200  
39 mg) solution in DMF (3 mL). The mixture was stirred at 30 °C for 18 h. The product was then  
40 dialyzed against deionized water for 24 h and freeze-dried to yield p(NβGlcEAM<sub>15</sub>-*b*-BA<sub>120</sub>)  
41 which was fully characterized by SEC, <sup>1</sup>H and <sup>19</sup>F NMR spectroscopy, and ATR-FTIR  
42 spectroscopy.  
43  
44  
45  
46  
47  
48  
49  
50  
51  
52  
53  
54  
55  
56  
57  
58  
59  
60

### *In vitro drug release from ampicillin-loaded glyco-NPs*

Ampicillin-encapsulated glyco-NPs were prepared using the nanoprecipitation method with the addition of 0.5 mg of ampicillin to the organic phase. Samples with a specific amount of ampicillin-encapsulated glyco-NP suspensions were subjected to high-speed centrifugation of 10,000 rpm for 30 min. The supernatant containing the unencapsulated ampicillin was isolated. The ampicillin content in the supernatant was assayed by HPLC and the encapsulation efficiency (EE) was calculated. Full details are given in the Supporting Information file.

### *Turbidimetric Assay*

Concanavalin A (Con A) was dissolved in HBS buffer (10 mM HEPES, 90 mM NaCl, 1 mM MgCl<sub>2</sub>, 1 mM CaCl<sub>2</sub>, 1 mM MnCl<sub>2</sub>, pH = 7.4) (1 mg/mL), and the resulting solution was gently mixed. Turbidity measurements were performed by adding the Con A solution (400 μL) to a dry quartz cuvette (500 μL volume, 1 cm path length). A solution of the glyco-NP of interest in HBS buffer (prepared by nanoprecipitation method as described above) was then added (100 μL at 2 mg/mL). Upon addition, the solution was mixed vigorously using a micropipette before placement in a Varian Cary-100 UV–Vis spectrophotometer. Absorbance data were recorded at 420 nm for 10 min.

### *Bacteriological experiments*

The bacteriological studies of the glyco-NPs (both Glc-NPs and Gal-NPs) and the ampicillin loaded glyco-NPs were investigated using an *Escherichia coli* K-12 wild-type strain (W3110 / ATCC27325, F<sup>-</sup>, λ<sup>-</sup>, *rpoS*(Am), *rph-1*, *Inv(rrnD-rrnE)*), *Staphylococcus aureus* (3R7089 strain

1  
2  
3 Oxford / ATCC9144) and *Staphylococcus epidermidis* (laboratory strain from clinical isolate) as  
4 representative Gram-negative (*E. coli*) and Gram-positive (*S. aureus* and *S. epidermidis*) species.  
5  
6 MIC was defined as the lowest concentration which completely inhibited bacterial growth after  
7  
8 incubation at 37°C for 16 h with agitation. Absorbance measurements at  $A_{650\text{nm}}$  were obtained  
9  
10 using a Biotek Synergy H4 Plate Reader. Full details are given in the Supporting Information  
11  
12 file.  
13  
14  
15  
16  
17  
18  
19

## 20 RESULTS AND DISCUSSION

21  
22 We designed amphiphilic glycopolymers with different compositions (hydrophilic to  
23 hydrophobic block ratio) that could assemble in aqueous solution, using the nanoprecipitation  
24 method,<sup>29, 30</sup> into NPs with sugar moieties presented on the surface. Our synthetic approach was  
25 based on the reversible addition fragmentation chain transfer (RAFT) polymerization of an  
26 activated ester, pentafluorophenyl acrylate (PFPA), followed by chain extension using n-butyl  
27 acrylate (BA) for subsequent modification with aminoethyl glycosides (Fig. 1A). We first  
28 polymerized PFPA using benzyl 2-hydroxyethyl carbonotrithioate (BHECTT) as a chain transfer  
29 agent. The resulting pPFPA macroRAFT agents were then used to polymerize BA to generate  
30 block copolymers with different compositions as revealed by <sup>1</sup>H-NMR spectroscopy (Fig. S1,  
31 supporting information). After purification by reprecipitation, the block copolymers were  
32 analyzed by SEC which showed monomodal distributions with dispersities of about ca. 1.2. The  
33 RAFT end group on the block copolymers was removed by treatment with azobisisobutyronitrile  
34 (AIBN). The block copolymers were subsequently modified by reaction with 2'-aminoethyl-β-D-  
35 glucopyranoside or 2'-aminoethyl-β-D-galactoside. Under optimized experimental conditions, a  
36 high yield with total consumption of pentafluorophenyl ester as revealed by <sup>1</sup>H- and <sup>19</sup>F-NMR and  
37  
38  
39  
40  
41  
42  
43  
44  
45  
46  
47  
48  
49  
50  
51  
52  
53  
54  
55  
56  
57  
58  
59  
60



FTIR spectroscopy were achieved (Fig. S2–4, supporting information). The final glycopolymers were characterized by SEC as shown in Table S1 (supporting information).

Glyco-NPs were prepared *via* the nanoprecipitation method and characterized by determining their diameter, external morphology and ampicillin encapsulation efficiency. The results showed that as the DP of the hydrophobic segment (pBA) increases, the diameter of the obtained NPs also increases (Table 1). Glucopolymer p(N $\beta$ GlcEAM<sub>15</sub>-*b*-BA<sub>120</sub>) was found to form the largest NPs with a diameter of 272  $\pm$  14 nm by DLS, Table 1. In addition, TEM was used to explore the morphology of the NPs. The obtained NPs are roughly spherical in shape; the apparent diameter of the NPs by TEM was found to be higher than their diameter in the hydrated state, most probably because of their flattened structure (Fig. 1B and 1F). Encapsulation of ampicillin led to a small increase in NP diameter (Table 1, entries 4 and 5). We therefore employed NPs made from glycopolymer p(N $\beta$ GlcEAM<sub>15</sub>-*b*-BA<sub>120</sub>) in this study which showed the largest diameter and were expected to possess the highest drug loading capacity. The ampicillin encapsulation efficiency (EE) of these NPs was found to be 47 %.

**Table 1.** DLS measurements for the obtained glyco-NPs.

Sample	Size by DLS (nm) $\pm$ SD	Polydispersity, PI $\pm$ SD
p(N $\beta$ GlcEAM <sub>15</sub> - <i>b</i> -BA <sub>30</sub> )	145 $\pm$ 2	0.219 $\pm$ 0.022
p(N $\beta$ GlcEAM <sub>15</sub> - <i>b</i> -BA <sub>45</sub> )	197 $\pm$ 6	0.229 $\pm$ 0.018
p(N $\beta$ GlcEAM <sub>15</sub> - <i>b</i> -BA <sub>75</sub> )	218 $\pm$ 8	0.227 $\pm$ 0.027
p(N $\beta$ GlcEAM <sub>15</sub> - <i>b</i> -BA <sub>120</sub> )	272 $\pm$ 14	0.234 $\pm$ 0.032
Ampicillin loaded p(N $\beta$ GlcEAM <sub>15</sub> - <i>b</i> -BA <sub>120</sub> )	302 $\pm$ 23	0.297 $\pm$ 0.026

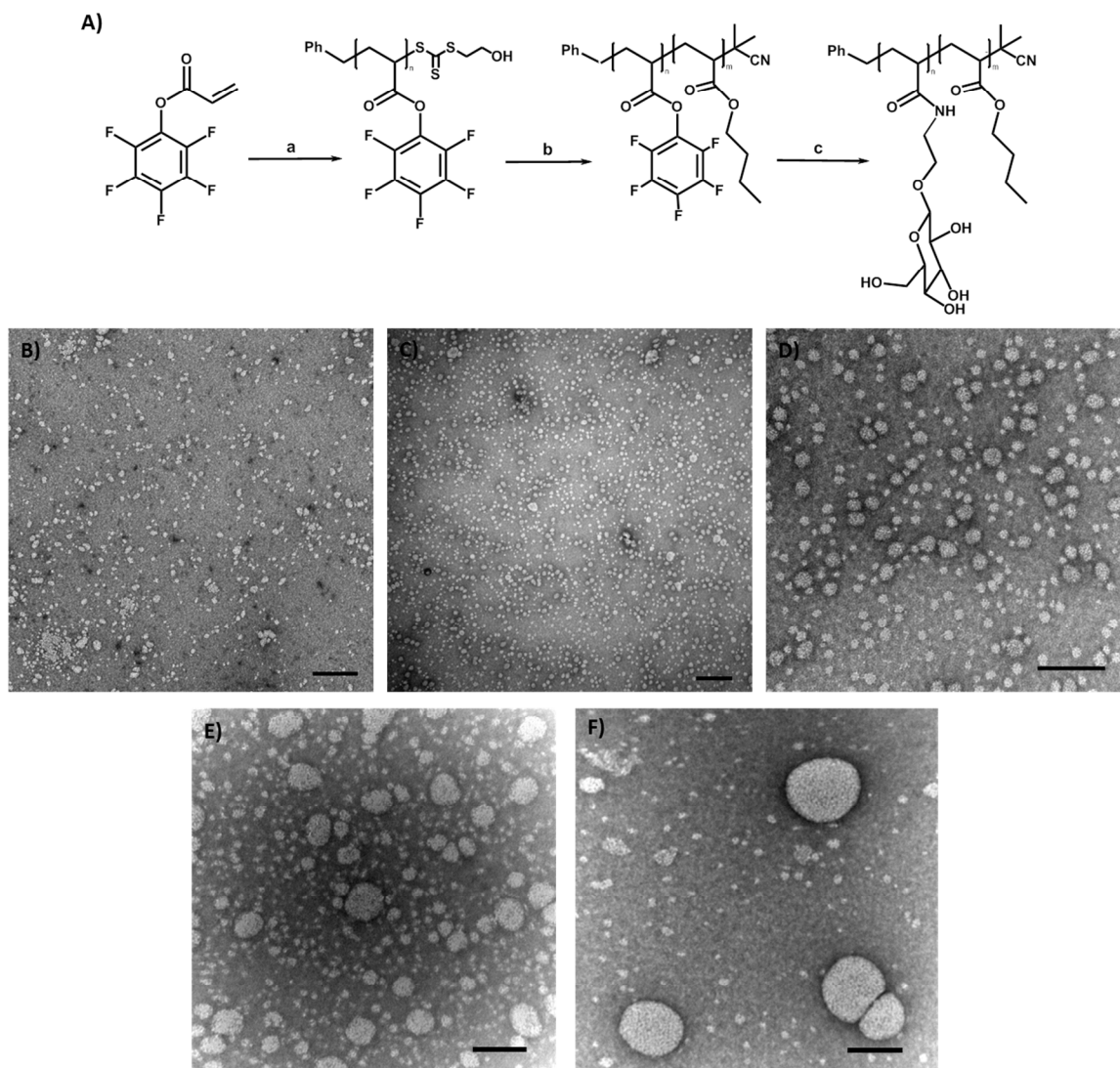


**Figure 1.** A) Schematic representation of amphiphilic glycopolymers synthesis (Conditions: a) BHECTT and AIBN in benzene at 70 °C for 6 h, b) BA and AIBN in benzene at 70 °C for 6 h followed excess AIBN at 70 °C for 6 h, c) 2'-aminoethyl-β-D-glucopyranoside and TEA in DMF-water at 30 °C for 18 h. B)-F) TEM images of glyco-NPs made from B) p(NβGlcEAM<sub>15</sub>-

b-BA<sub>30</sub>), C) p(NβGlcEAM<sub>15</sub>-*b*-BA<sub>45</sub>), D) p(NβGlcEAM<sub>15</sub>-*b*-BA<sub>75</sub>), E) p(NβGlcEAM<sub>15</sub>-*b*-BA<sub>120</sub>), and F) ampicillin loaded glyco-NPs made from P(NβGlcEAM<sub>15</sub>-*b*-BA<sub>120</sub>). Scale bar = 200 nm.

The typical *in vitro* release profile of a drug from NPs often displays two distinct regions; an early, rapid release, while the remainder is liberated slowly during an extended period of time. The early release represents the loss of surface-associated and poorly entrapped drug. The magnitude of this burst effect is dependent on the quantity of drug bound to the outer surface of the NPs. However, the drug release from within the NP core is controlled by diffusion.<sup>31</sup> In our case, the percentage cumulative ampicillin release versus time plot did not show an initial burst release phase. Instead, slow and constant zero-order ampicillin release kinetics was observed. The cumulative ampicillin release from NPs after 21 days was found to be 56 % (Fig. 2).

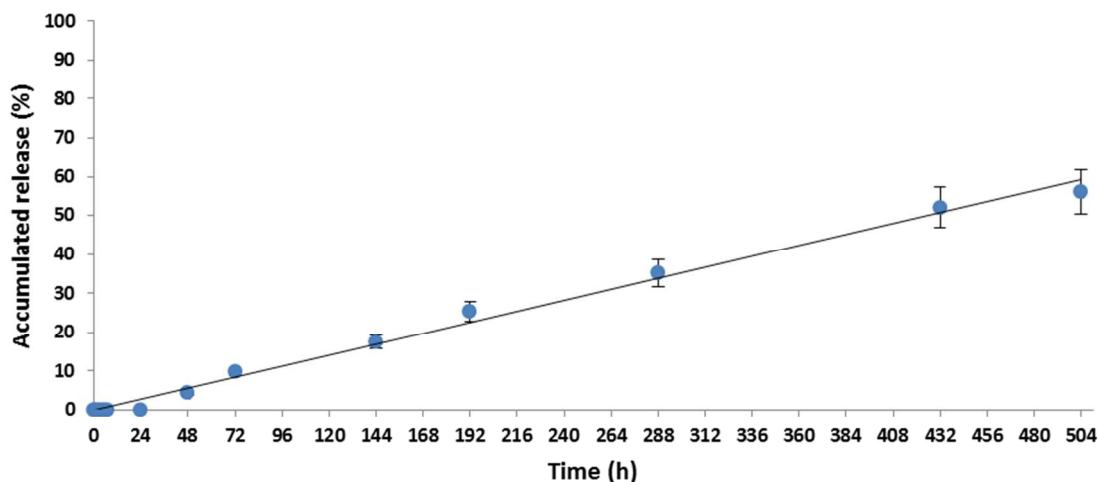


**Figure 2.** *In vitro* release profile of ampicillin-loaded P(NβGlcEAM<sub>15</sub>-*b*-BA<sub>120</sub>) glyco-NPs in PBS (pH 7.4) at 37 °C.

1  
2  
3 The ability of the glycosylated NPs to bind to the glucose/mannose specific lectin  
4 Concanavalin-A (Con-A) was evaluated using a well-established turbidimetric assay.<sup>32</sup> In this  
5  
6  
7  
8 assay, the Con-A tetramer is mixed with an excess of the multivalent ligand under investigation,  
9  
10 inducing rapid precipitation. The change in turbidity is related directly to the formation of Con-A  
11  
12 clusters in solution mediated by the appropriate multivalent ligand. The glucose-containing NPs  
13  
14 were found to bind readily to Con-A; however, galactose-containing NPs did not show any  
15  
16 binding affinity (Fig. 3). These results indicate that D-glucose moieties are presented on the  
17  
18 surface of the NPs in a densely multivalent manner and are available for lectin binding. These  
19  
20 results also show the potential of the glyco-NPs to bring about targeted delivery to cells  
21  
22 displaying glucosyl-binding lectins.  
23  
24  
25  
26  
27  
28  
29  
30  
31  
32  
33  
34  
35  
36  
37  
38  
39  
40  
41  
42  
43  
44  
45  
46  
47  
48  
49  
50  
51  
52  
53  
54  
55  
56  
57  
58  
59  
60

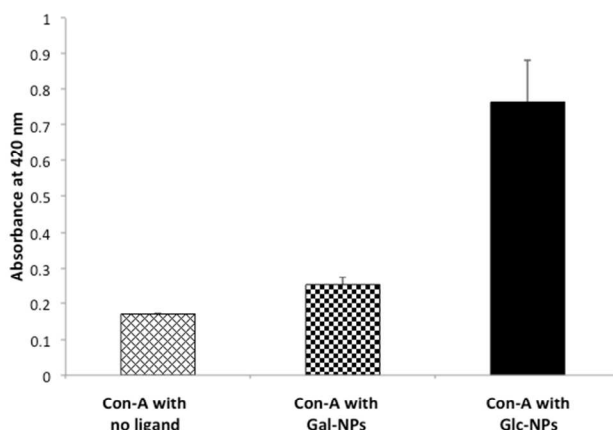


**Figure 3.** Assessment of the binding of NPs to Con-A by turbidimetry, from left to right: Con-A alone (control); Con-A plus glucosylated nanoparticles; Con-A plus galactosylated nanoparticles.

We performed bacterial minimal inhibitory concentration (MIC) assays<sup>33</sup> using both glucosylated and galactosylated NPs (Glc-NPs and Gal-NPs, respectively), ampicillin loaded

1  
2  
3 Glc-NPs and free ampicillin against representative Gram-positive (*Staphylococcus aureus* and  
4  
5 *Staphylococcus epidermidis*) and Gram-negative (*Escherichia coli*) bacteria. Unloaded Glc-NPs  
6  
7 and Gal-NPs showed no significant antibacterial activity against these bacterial species (Fig. 4A-  
8  
9 C), although there was some indication of a reduction in growth in the 5-25  $\mu\text{g/ml}$  concentration  
10  
11 range for Glc-NPs mixed with *E. coli* (Fig. 4A). Visual inspection of the plates revealed that this  
12  
13 is due to aggregation of *E. coli* correlating with an increased Glc-NP concentration (Fig. 4D and  
14  
15 also evident in the increased absorbance at the highest Gal-NP concentrations in Fig. 4A) (no  
16  
17 aggregation was evident in any other wells). Carbohydrate recognition sites have been identified  
18  
19 on the pili of *E. coli*. The FimH protein, present in the W3110 strain used here<sup>34</sup> which is  
20  
21 exposed at the tip of the pili, has binding specificity for glucose and mannose on human cell  
22  
23 surfaces<sup>18</sup> and so this is a likely explanation for the *E. coli* aggregation observed with Glc-NPs  
24  
25 but not with the non-binding Gal-NPs. The affinity of FimH for galactose is 10-fold lower than  
26  
27 that for glucose in a surface plasmon resonance assay<sup>35</sup>.  
28  
29  
30  
31  
32  
33  
34  
35  
36  
37  
38  
39  
40  
41  
42  
43  
44  
45  
46  
47  
48  
49  
50  
51  
52  
53  
54  
55  
56  
57  
58  
59  
60

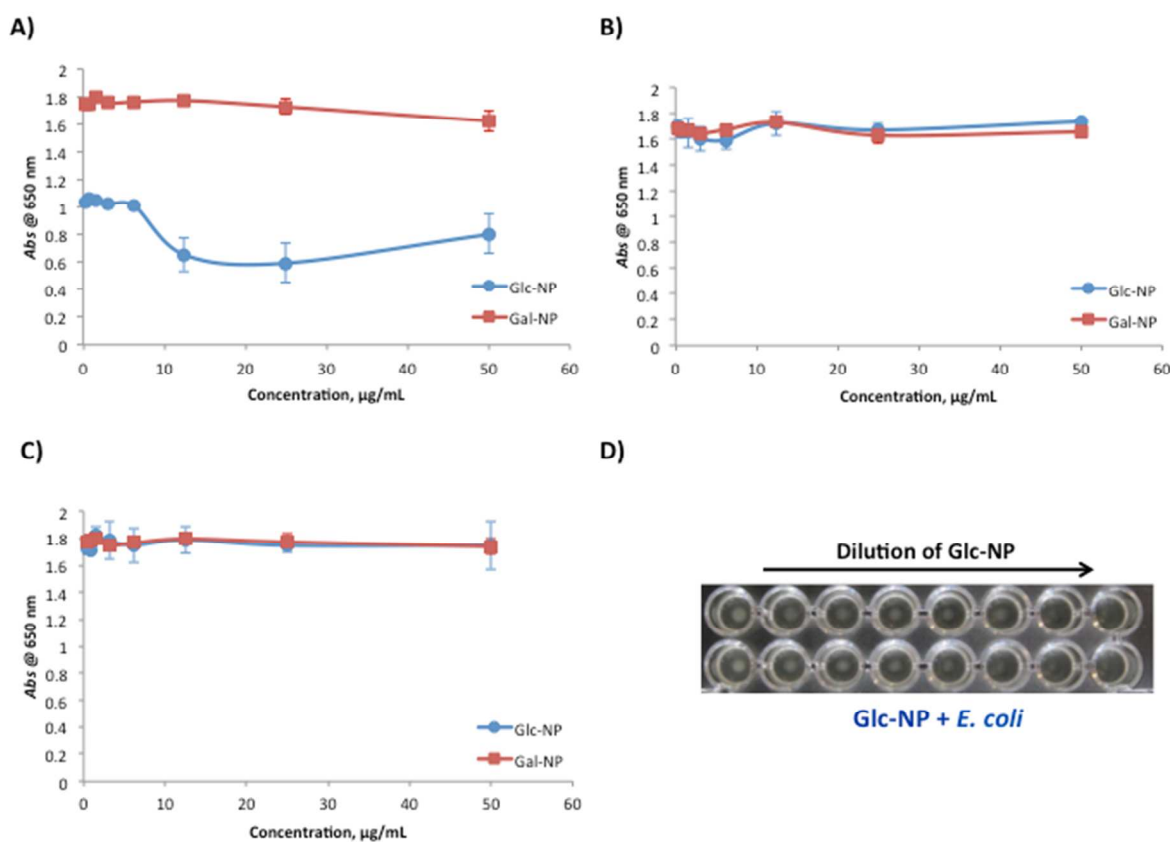


**Figure 4.** Evaluation of the growth and aggregation of bacteria in the presence of glucosylated nanoparticles (blue circles) and galactosylated nanoparticles (red squares): A) *E. coli*, B) *S. aureus*, C) *S. epidermidis*. D) Section of a 96-well plate showing bacterial aggregation of *E. coli* as a consequence of incubation with glucosylated nanoparticles for 16 h.

Representative examples of bacterial cultures grown in liquid media in the presence of Glc-NPs or ampicillin loaded Glc-NPs are shown in Fig. 5A (the results for *E. coli* only are shown, although similar results were obtained with *S. aureus* and *S. epidermidis*). Bacterial growth is evident in liquid media and in the presence of Glc-NPs (Fig. 5A, left and centre), while inclusion of ampicillin in the NPs completely inhibited the bacterial growth (Fig. 5A, right).

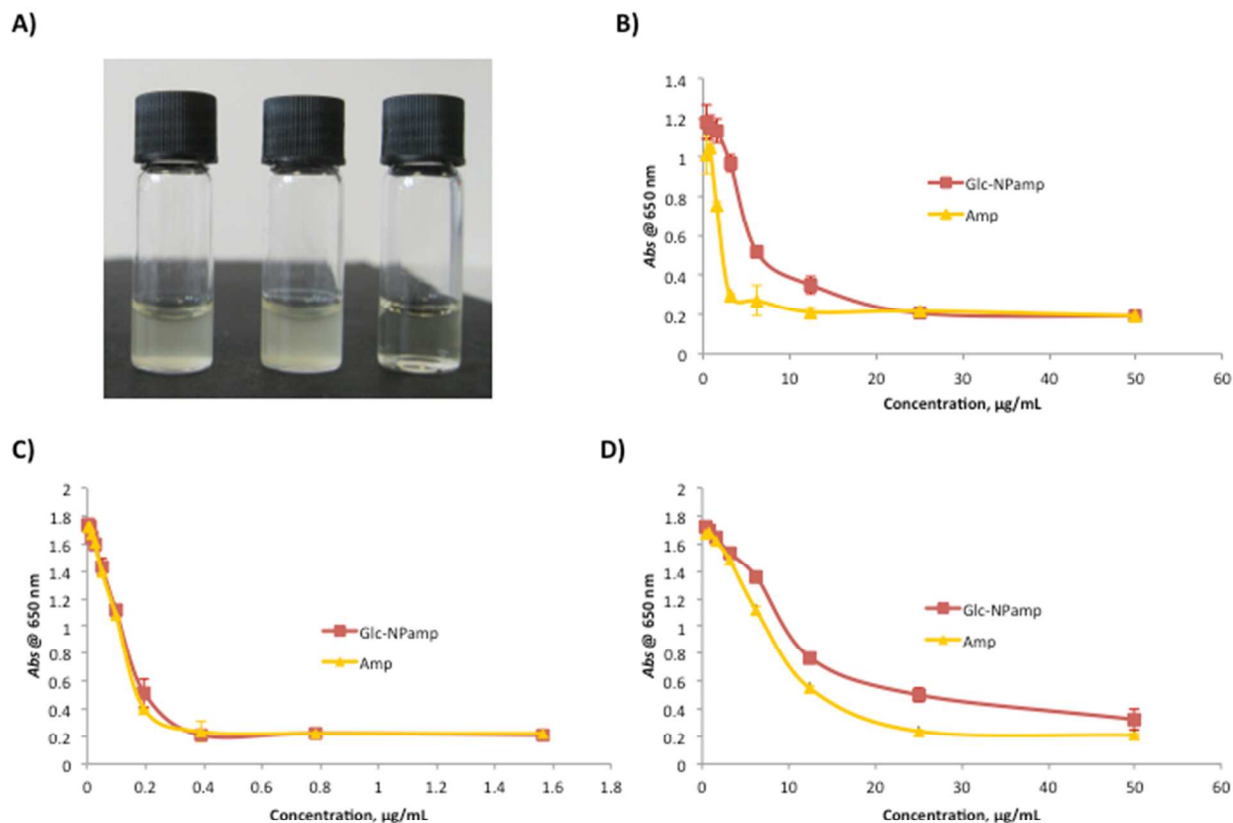


**Figure 5.** A) *E. coli* grown in liquid media (left), in the presence of Glc-NPs (centre) and ampicillin loaded Glc-NPs (right). Evaluation of bacterial growth in the presence of ampicillin loaded Glc-NPs (red squares) and ampicillin (yellow triangles). B) *E. coli*, C) *S. aureus*, D) *S. epidermidis*.

Both ampicillin-loaded Glc-NPs and free ampicillin show antibacterial activity against *E. coli*, *S. aureus* and *S. epidermidis* (Fig. 5B-D). The MIC values of ampicillin loaded Glc-NPs and free ampicillin against different bacterial strains are shown in Table 2. Ampicillin-loaded Glc-NPs exhibited MICs 4-fold and 2-fold higher than free ampicillin against the Gram-negative strain *E.*

1  
2  
3 *coli* and Gram-positive strains *S. epidermidis* and *S. aureus*, respectively. This presumably  
4 reflects the slower release of ampicillin from the Glc-NPs, compared to free ampicillin. The  
5 extent of bacterial killing is nonetheless quite remarkable given the small amount of ampicillin  
6 released over the 16h timeframe of the bacterial culture experiments (Fig. 2). The Glc-NPs alone  
7 display some antibacterial effect even without encapsulation of ampicillin, the reason for which  
8 requires further investigation.  
9  
10  
11  
12  
13  
14  
15  
16  
17  
18  
19

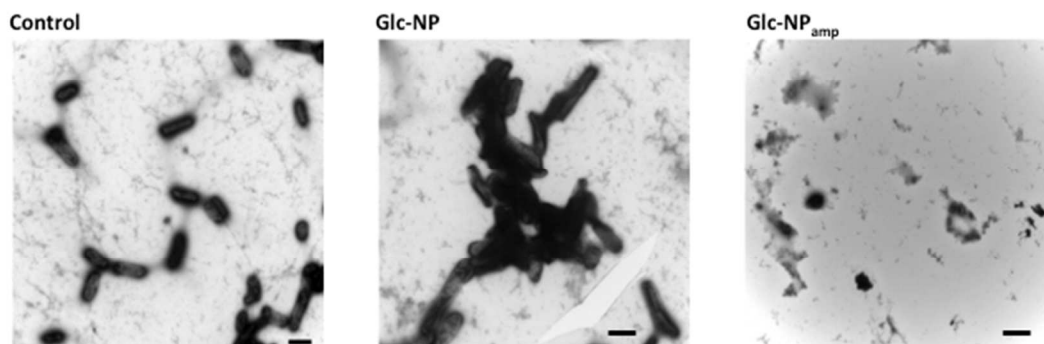
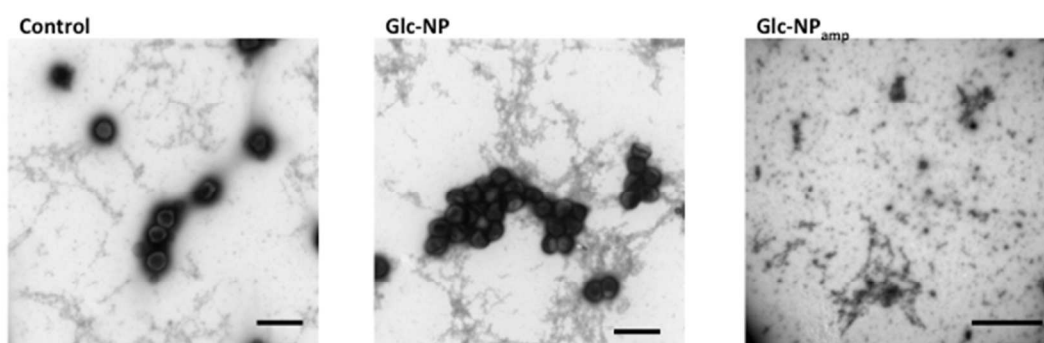
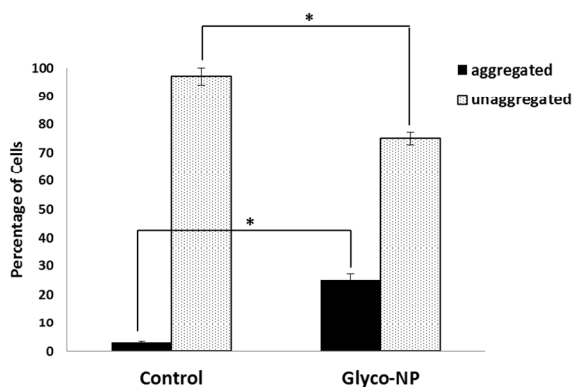
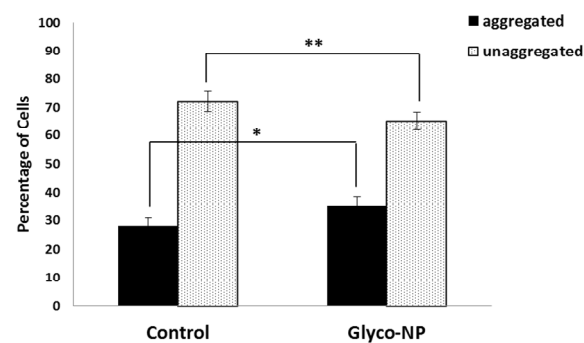
20 **Table 2.** MIC assays on *E. coli*, *S. epidermidis* and *S. aureus*.  
21  
22

23 <b>Strain</b>	24 <b>Glc-NP</b>	25 <b>Glc-NP<sub>amp</sub></b>	26 <b>Free Ampicillin</b>
	( $\mu\text{g mL}^{-1}$ )	( $\mu\text{g mL}^{-1}$ )	( $\mu\text{g mL}^{-1}$ )
27 <i>E. coli</i>	25	6.25	1.56
28 <i>S. epidermidis</i>	—	25	12.5
29 <i>S. aureus</i>	—	0.196	0.098

30  
31  
32  
33  
34

35 We also investigated bacterial morphology and aggregation in the presence or absence of Glc-  
36 NPs using TEM (Fig. 6A and 6B). The bacterial cultures were dried onto TEM grids, stained  
37 with uranyl acetate, and imaged using TEM. The resulting micrographs confirm that bacteria in  
38 the presence of Glc-NPs form significantly more aggregates compared to the control experiment  
39 without addition of Glc-NPs. Indeed, these TEM micrographs are representative of each sample  
40 as indicated by the collected statistical data (Fig. 6C and 6D).  
41  
42  
43  
44  
45  
46  
47  
48  
49  
50  
51  
52  
53  
54  
55  
56  
57  
58  
59  
60



A) *E. coli*B) *S. aureus*C) *E. coli*D) *S. aureus*

**Figure 6.** TEM images showing A) *E. coli* and B) *S. aureus* in the presence or absence of Glc-NPs. Cells were stained with uranyl acetate. Quantification of bacterial aggregation from TEM images for C) *E. coli* and D) *S. aureus* cells in the presence or absence of Glc-NPs. \* denotes  $p$

1  
2  
3 value < 0.15; \*\*  $p$  value < 0.0001 as determined by Student's  $t$  test (15 fields of view per  
4  
5  
6 experiment)  
7  
8  
9

10  
11 We refer to any cluster of ten or more cells attached to each other as “aggregated”; fewer than  
12  
13 ten associated cells was defined as “unaggregated”. Based on this collected data, we noted a  
14  
15 marked increase in the aggregation percent of *E. coli* cells in the presence of Glc-NPs compared  
16  
17 to the control experiment without Glc-NPs (Fig. 6C). This was also the case for *S. aureus* cells  
18  
19 (Fig. 6D), although the difference between the aggregation percentage of cells in the presence of  
20  
21 Glc-NPs and in their absence (control) was much less obvious. The suggested explanation for *E.*  
22  
23 *coli* aggregation is the presence of the Glc-binding FimH protein present on the tips of the  
24  
25 bacterial pili. No such Glc-binding protein has been identified for *S. aureus*, so the significant  
26  
27 ability of the Glc-NPs to aggregate these bacteria is as yet unexplained. These results are  
28  
29 consistent with the MIC and culture assays presented earlier. We suggest that this bacterial  
30  
31 aggregation induced by the glyconanobiotics accounts for their antibacterial effect, perhaps by  
32  
33 facilitating release or delivery of the encapsulated antibiotic.  
34  
35  
36  
37  
38  
39  
40

## 41 CONCLUSIONS

42  
43  
44 In this study, glycosylated polymeric nanoparticles (glyco-NPs) composed of a poly(n-butyl  
45  
46 acrylate) (pBA) core and a poly(N-2-( $\beta$ -D-Glucosyloxy)ethyl acrylamide) (pN $\beta$ GlcEAM) corona  
47  
48 were prepared by nanoprecipitation in PBS of preformed RAFT block copolymers. The  
49  
50 antibiotic ampicillin was encapsulated in the core of these glycosylated NPs and released  
51  
52 following a zero-order kinetic profile. The glycopolymer chains were presented to the outside  
53  
54 environment of the NP and could bind specifically to the lectin Con A. The glycosylated NPs  
55  
56  
57  
58  
59  
60

1  
2  
3 were bioactive, exhibiting significant adhesive interactions with several bacterial strains (*E. coli*,  
4 *S. epidermidis* and *S. aureus*) as judged by the ability to induce bacterial aggregation. In the case  
5  
6 of *E. coli*, glucosylated NPs were able to induce substantial bacterial aggregation compared to  
7  
8 the galactosylated analogues. The ability of our glycosylated NPs to display the dual function of  
9  
10 bacterial aggregation and antibiotic delivery is potentially a powerful route to produce  
11  
12 antimicrobials with improved efficacy. Indeed, it was found that bacterial killing abilities only  
13  
14 slightly lower than that of free ampicillin were obtained, despite the much lower instantaneous  
15  
16 concentration of antibiotic in the vicinity of the glyco-NPs. By tuning the carbohydrate epitope  
17  
18 on the NP tethers through polymer design and hence affinities in cell aggregation, a new class of  
19  
20 *glyconanobiotics* may emerge.  
21  
22  
23  
24  
25  
26  
27  
28

## 29 ASSOCIATED CONTENT

30  
31  
32 **Supporting Information.** Materials and instrumentation used; detailed experimental  
33  
34 procedures; characterization data for block glycopolymers; calculation of ampicillin  
35  
36 encapsulation efficiency. This information is available free of charge on the ACS Publications  
37  
38 website at DOI: xxxx.  
39  
40  
41  
42  
43

## 44 AUTHOR INFORMATION

### 45 46 47 **Corresponding Authors**

48  
49  
50 \*E-mail: [neil.cameron@monash.edu](mailto:neil.cameron@monash.edu)

51  
52  
53 \*E-mail: [a.m.eissa@warwick.ac.uk](mailto:a.m.eissa@warwick.ac.uk)

### 54 55 56 57 **Author Contributions**

1  
2  
3 The manuscript was written through contributions of all authors. All authors have given approval  
4  
5  
6 to the final version of the manuscript.  
7

## 8 9 **Notes**

10  
11 The authors declare no competing financial interests.  
12  
13  
14  
15  
16

## 17 **ACKNOWLEDGEMENTS**

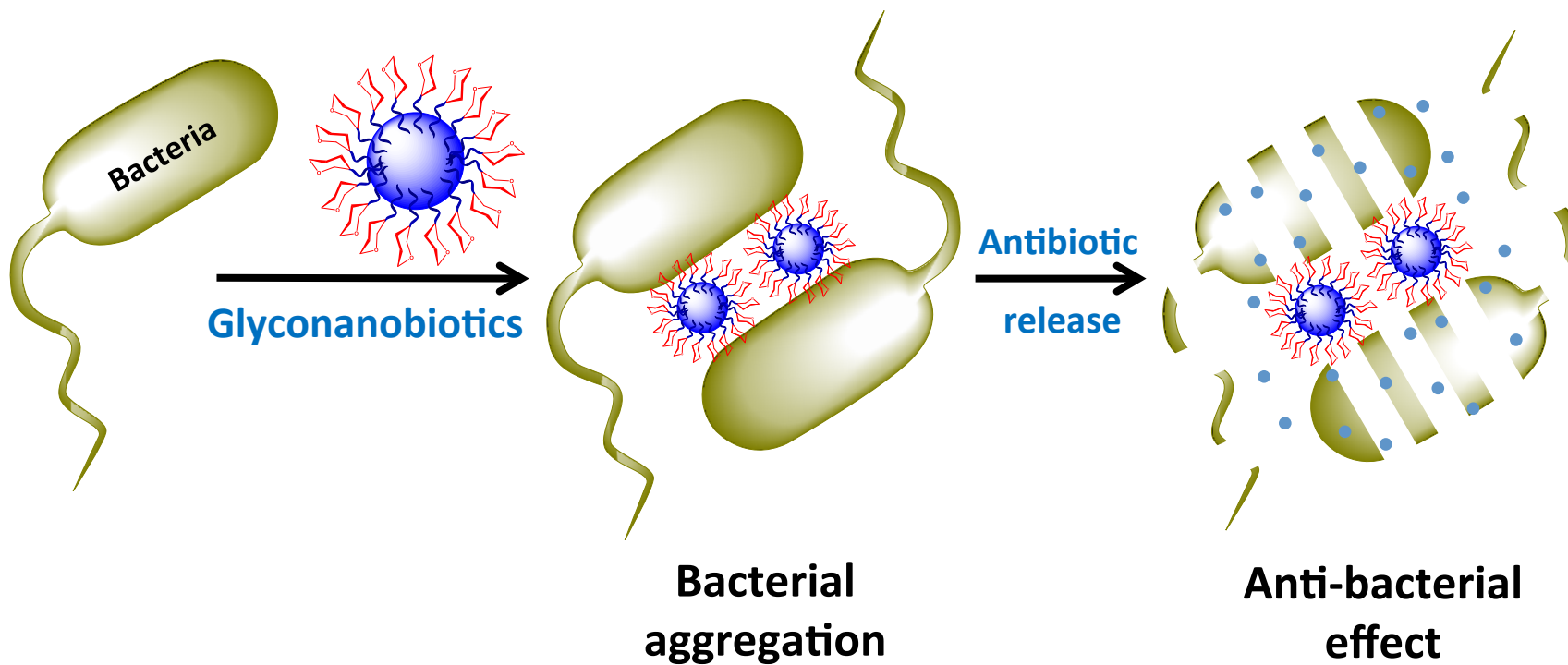
18  
19  
20 The Leverhulme Trust is thanked for funding (F/00128/BO).  
21  
22  
23  
24  
25

## 26 **REFERENCES**

- 27  
28  
29 1. Cohen, M. L., *Nature* **2000**, *406*, 762-767.  
30  
31 2. Walsh, C., *Nature* **2000**, *406*, 775-781.  
32  
33 3. Taylor, P. W.; Stapleton, P. D.; Luzio, J. P., *Drug Discovery Today* **2002**, *7*, 1086-1091.  
34  
35 4. Miller, K. P.; Wang, L.; Benicewicz, B. C.; Decho, A. W., *Chem. Soc. Rev.* **2015**, *44*,  
36  
37 7787-7807.  
38  
39 5. Schrand, A. M.; Rahman, M. F.; Hussain, S. M.; Schlager, J. J.; Smith, D. A.; Ali, S. F.,  
40  
41 *Wiley Interdiscip. Rev.: Nanomed. Nanobiotechnol.* **2010**, *2*, 544-568.  
42  
43 6. Rizzello, L.; Cingolani, R.; Pompa, P. P., *Nanomedicine* **2013**, *8*, 807-821.  
44  
45 7. Abed, N.; Couvreur, P., *Int. J. Antimicrob. Agents* **2014**, *43*, 485-496.  
46  
47 8. Seil, J. T.; Webster, T. J., *Int. J. Nanomed.* **2012**, *7*, 2767-2781.  
48  
49 9. Zopf, D.; Roth, S., *Lancet* **1996**, *347*, 1017-1021.  
50  
51 10. Ofek, I.; Hasy, D. L.; Sharon, N., *FEMS Immunol. Med. Microbiol.* **2003**, *38*, 181-191.  
52  
53 11. Bavington, C.; Page, C., *Respiration* **2005**, *72*, 335-344.  
54  
55  
56  
57  
58  
59  
60

- 1
- 2
- 3 12. Kunz, C.; Rudloff, S.; Baier, W.; Klein, N.; Strobel, S., *Annu. Rev. Nutr.* **2000**, *20*, 699-
- 4 722.
- 5
- 6
- 7
- 8 13. Xue, X.; Pasparakis, G.; Halliday, N.; Winzer, K.; Howdle, S. M.; Cramphorn, C. J.;
- 9 Cameron, N. R.; Gardner, P. M.; Davis, B. G.; Fernandez-Trillo, F.; Alexander, C.,
- 10 *Angew. Chem.-Int. Ed.* **2011**, *50*, 9852-9856.
- 11
- 12
- 13
- 14
- 15 14. Ramstrom, O.; Yan, M. D., *Chem.-Eur. J.* **2015**, *21*, 16310-16317.
- 16
- 17
- 18 15. Ramtenki, V.; Raju, D.; Mehta, U. J.; Ramana, C. V.; Prasad, B. L. V., *New J. Chem.*
- 19 **2013**, *37*, 3716-3720.
- 20
- 21
- 22 16. Tseng, Y. T.; Chang, H. T.; Chen, C. T.; Chen, C. H.; Huang, C. C., *Biosens. Bioelectron.*
- 23 **2011**, *27*, 95-100.
- 24
- 25
- 26
- 27 17. Kumar, C. G.; Sujitha, P., *Nanotechnology* **2014**, *25*.
- 28
- 29 18. Pieters, R. J., *Med. Res. Rev.* **2007**, *27*, 796-816.
- 30
- 31 19. Oliyai, R.; Lindenbaum, S., *Int. J. Pharm.* **1991**, *73*, 33-36.
- 32
- 33
- 34 20. Mandell, G. L.; Douglas, R. G. J.; Bennett, J. E., *Principles and Practice of Infectious*
- 35 *Diseases Third Edition*. Elsevier, Philadelphia, PA, 1990.
- 36
- 37
- 38 21. Ahren, I. L.; Karlsson, E.; Forsgren, A.; Riesbeck, K., *J. Antimicrob. Chemother.* **2002**,
- 39 *50*, 903-906.
- 40
- 41
- 42
- 43 22. Rothbard, J. B.; Wender, P. A.; McGrane, P. L.; Sista, L. V. S.; Kirschberg, T. A., US
- 44 Pat. 08623833, 2014.
- 45
- 46
- 47 23. Schumacher, I.; Margalit, R., *J. Pharm. Sci.* **1997**, *86*, 635-641.
- 48
- 49 24. Huh, A. J.; Kwon, Y. J., *J. Controlled Release* **2011**, *156*, 128-145.
- 50
- 51 25. Bakkerwoudenberg, I., *Adv. Drug Delivery Rev.* **1995**, *17*, 5-20.
- 52
- 53 26. Mora-Huertas, C. E.; Fessi, H.; Elaissari, A., *Int. J. Pharm.* **2010**, *385*, 113-142.
- 54
- 55
- 56
- 57
- 58
- 59
- 60

- 1  
2  
3  
4  
5  
6  
7  
8  
9  
10  
11  
12  
13  
14  
15  
16  
17  
18  
19  
20  
21  
22  
23  
24  
25  
26  
27  
28  
29  
30  
31  
32  
33  
34  
35  
36  
37  
38  
39  
40  
41  
42  
43  
44  
45  
46  
47  
48  
49  
50  
51  
52  
53  
54  
55  
56  
57  
58  
59  
60
27. Eissa, A. M.; Cameron, N. R., Glycopolymer Conjugates. In *Bio-Synthetic Polymer Conjugates*, Schlaad, H., Ed. 2013; *Adv. Polym. Sci.* Vol. 253, pp 71-114.
28. Eissa, A. M.; Smith, M. J. P.; Kubilis, A.; Mosely, J. A.; Cameron, N. R., *J. Polym. Sci. Pt. A-Polym. Chem.* **2013**, *51*, 5184-5193.
29. Barichello, J. M.; Morishita, M.; Takayama, K.; Nagai, T., *Drug Dev. Ind. Pharm.* **1999**, *25*, 471-476.
30. Zili, Z.; Sfar, S.; Fessi, H., *Int. J. Pharm.* **2005**, *294*, 261-267.
31. Xiong, X. Y.; Li, Y. P.; Li, Z. L.; Zhou, C. L.; Tam, K. C.; Liu, Z. Y.; Xie, G. X., *J. Controlled Release* **2007**, *120*, 11-17.
32. Cairo, C. W.; Gestwicki, J. E.; Kanai, M.; Kiessling, L. L., *J. Am. Chem. Soc.* **2002**, *124*, 1615-1619.
33. Andrews, J. M., *J. Antimicrob. Chemother.* **2001**, *48*, 5-16.
34. Hayashi, K.; Morooka, N.; Yamamoto, Y.; Fujita, K.; Isono, K.; Choi, S.; Ohtsubo, E.; Baba, T.; Wanner, B. L.; Mori, H.; Horiuchi, T., *Mol. Syst. Biol.* **2006**, *2*, 20060007.
35. Bouckaert, J.; Berglund, J.; Schembri, M.; De Genst, E.; Cools, L.; Wuhrer, M.; Hung, C. S.; Pinkner, J.; Slattegard, R.; Zavialov, A.; Choudhury, D.; Langermann, S.; Hultgren, S. J.; Wyns, L.; Klemm, P.; Oscarson, S.; Knight, S. D.; De Greve, H., *Mol. Microbiol.* **2005**, *55*, 441-55.



1  
2  
3  
4  
5  
6  
7  
8  
9  
10  
11  
12  
13  
14  
15  
16  
17  
18  
19  
20  
21  
22  
23  
24  
25  
26  
27  
28  
29  
30  
31  
32  
33  
34  
35  
36  
37  
38  
39  
40  
41  
42  
43  
44  
45  
46  
47